

Mixture Diffusion of Sulfonated Dyes into Cellulose Membrane. I. Application of Parallel Diffusion Model to Binary System of Acid Dyes with Small Affinity onto Cellulose

MASAKO MAEKAWA, MIWA OHMORI

Division of Life Science and Human Technology, Nara Women's University, Nara, 630 Japan

Received 3 February 1997; accepted 15 May 1997

ABSTRACT: Transport phenomena of a binary mixture of dyes with a small affinity onto cellulose into a water-swollen cellulose membrane were studied at 55°C. The results were analyzed on the basis of a parallel transport theory of surface and pore diffusion. The diffusion of dye molecules in a binary dye system could be described by the parallel diffusion model. Although existence of the other dye decreased the equilibrium adsorption of both dyes onto cellulose, the surface and pore diffusivities for the model of both dyes were same as those in the single dye system. © 1997 John Wiley & Sons, Inc. *J Appl Polym Sci* **66**: 2175–2181, 1997

Key words: mixture diffusion; sulfonated dyes; cellulose membrane; parallel transport theory; diffusivity

INTRODUCTION

Many studies have reported the equilibrium adsorption and diffusion of dyes from an aqueous solution of a binary dye mixture into cellulose.^{1–6} A complicated behavior of dyes for adsorption and diffusion is expected in a binary dye system due to the competition of the available surface on the substrate by dyes, change of the activity of each dye, and the complex formation between different dyes and so on.

In our previous articles,^{7–13} we reported the diffusion of a single dye system, i.e., the diffusion behavior of various sulfonated dyes into the water-swollen cellulose membrane was investigated and analyzed on the basis of a parallel diffusion model consisting of surface and pore diffusion. It was revealed that diffusion of the dyes could be described by the parallel diffusion model, in which

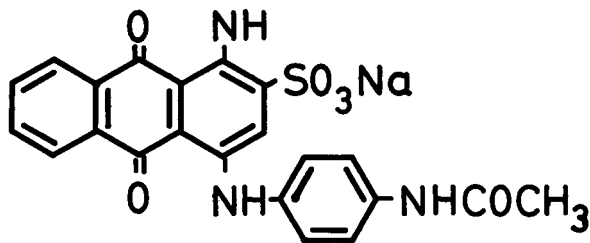
dye molecules diffuse in parallel both on the inner surface of the pores of cellulose in the adsorbed state (surface diffusion) and in the liquid phase of the water-filled pores of cellulose (pore diffusion); in addition, the surface diffusivity of the model correlates with an affinity of the dyes and the pore diffusivity of the model correlates with the molecular weight of the dyes with exceptions. In the present article, an attempt was made to apply the parallel diffusion model to a binary mixture of dyes with a small affinity onto cellulose, in which the factors that introduce the complicated behavior mentioned above are the least.

EXPERIMENTAL

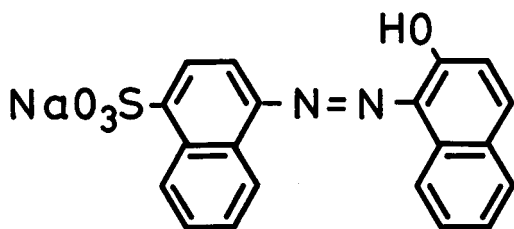
Materials

Sulfonated monoazo dyes, C.I. Acid Blue 40 (MW = 473.4) supplied by the Sumitomo Chemical Co. and C.I. Acid Red 88 (MW = 400.4) obtained from the Tokyo Kasei Co., were purified by column

Correspondence to: M. Maekawa.



C.I. Acid Blue 40



C.I. Acid Red 88

Figure 1 The structural formulas of the dyes.

chromatography and the Robinson and Mills' method,¹⁴ respectively. The structural formulas of the dyes are shown in Figure 1. Sodium chloride was obtained from the Nacalai Tesque Co. The cellulose membrane (cellophane film) supplied by the Rengo Co. was soaked in boiled deionized distilled water for 3 h (30 min \times 6 times) and then washed with deionized distilled water. The thickness of the water-swollen membrane (l) was 38.6 μm as measured by a membrane-thickness meter (Kohbunshi Keiki Co.). The void fraction (ϵ_p) and the volume per unit dry cellulose (V) in a water-swollen state were 0.733 and 2.38 dm^3/kg , respectively, as measured by the pycnometric method.⁸

Diffusion of the Dye-Adsorption Isotherms

Equilibrium isotherms for the adsorption of the dyes onto the cellulose membrane were measured by the batch method. The concentrations of both dyes in a bulk solution (C_0) for mixture dyeing were equal and 0.05–1 mol/m^3 . Sodium chloride was added at 50–150 mol/m^3 . The equilibrium for the single dyeing of AB40 or AR88 was attained in

1 or 2 h at 55°C, respectively. The equilibrium for the mixture dyeing of AB40 and AR88 was attained in 2 h at 55°C.

Adsorption rates were measured using an ultrafiltration-type cell with a water jacket (Sartorius SM165 26). The membrane was placed on a plastic plate at the bottom of the cell to establish non-steady-state diffusion as described elsewhere.⁷ Uptake curves were generated by the integral step method using one sheet of the membrane. The amount of the dye adsorbed over a given period was determined by the desorption of the dye from the membrane with 25% aqueous pyridine and by measuring its concentration using a Hitachi U-3200 spectrophotometer with 25% pyridine as a reference. The absorption spectra of the dye mixture in 25% aqueous pyridine were additive. Experiments were carried out at 55°C.

THEORETICAL

In the theoretical development of the diffusion equations, it is assumed that (1) the surface and pore diffusion occur in parallel within a cellulose membrane, (2) pore and surface diffusivities are constant during the adsorption process, (3) the pore diameter and the void fraction of the membrane are constant during the adsorption process, (4) the concentration of the dye anions in the pores is in local equilibrium with the concentration of adsorbed dye anions on the surface of the pore wall, and (5) the diffusion of sodium chloride is complete before significant diffusion of the dye molecules.

These assumptions lead to the following mass balance equation:

$$\epsilon_p \frac{\partial C}{\partial t} + \frac{\partial q}{\partial t} = \epsilon_p D_p \frac{\partial^2 C}{\partial z^2} + D_s \frac{\partial^2 q}{\partial z^2} \quad (1)$$

where C and q are the concentrations of the dye in the pores and on the surface of the pore wall, respectively (mol/m^3). t (s) and z (m) represent the time and distance through the membrane. ϵ_p is the void fraction of the pores. D_p and D_s represent the pore and surface diffusivities, respectively (m^2/s). Using the dimensionless variables defined in eq. (2), eq. (1) can be transformed to give eq. (3):

$$\tau_p = \frac{D_p t}{l^2}, \quad \rho = \frac{z}{l}, \quad x = \frac{C}{C_0}, \quad y = \frac{q}{q_0},$$

$$\alpha = \frac{q_0}{\epsilon_p C_0}, \quad \beta = \alpha \frac{D_s}{D_p} \quad (2)$$

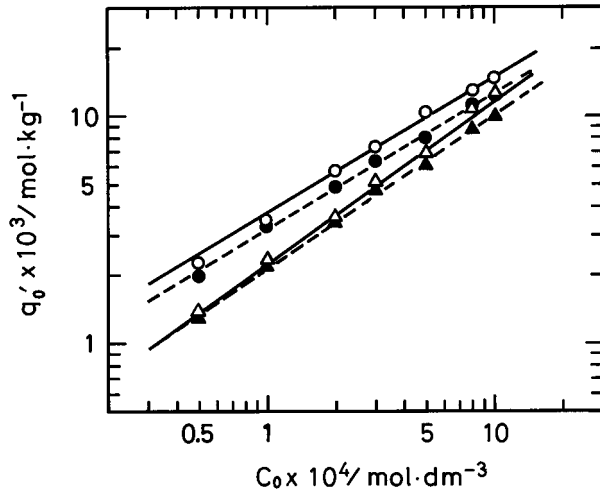


Figure 2 Effects of mixture dyeing on adsorption isotherms of C.I. Acid Blue 40 (AB40) and C.I. Acid Red 88 (AR88) on a cellulose membrane in the presence of 100 mol/m³ of NaCl at 55°C. (○) AR88 single¹¹; (△) AB40 single; (●) AR88 in the presence of AB40; (▲) AB40 in the presence of AR88.

$$\frac{\partial x}{\partial \tau_p} + \alpha \frac{\partial y}{\partial \tau_p} = \frac{\partial^2 x}{\partial \rho^2} + \beta \frac{\partial^2 y}{\partial \rho^2} \quad (3)$$

where C_0 is the dye concentration in the bulk solution and q_0 is the adsorbed concentration of the dye in equilibrium with C_0 (mol/m³). There are two limiting cases: $\beta = 0$ (pore diffusion control) and $\beta = \infty$ (surface diffusion control). However, eq. (3) cannot be solved for $\beta = \infty$, and, hence, eq. (1) is transformed to eq. (4):

$$\frac{\partial x}{\partial \tau_s} + \alpha \frac{\partial y}{\partial \tau_s} = \alpha \frac{\partial^2 y}{\partial \rho^2} \quad (\text{surface diffusion control}) \quad (4)$$

where $\tau_s = D_s t / l^2$. The relation between x and y is calculated according to the equilibrium isotherm (fourth assumption). Applying the Freundlich isotherm defined by eq. (5), we transformed eqs. (3) and (4) into eqs. (6) and (7), respectively:

$$y = x^\gamma \quad (5)$$

$$\left[\alpha + \frac{1}{\gamma} y^{(1-\gamma)/\gamma} \right] \frac{\partial y}{\partial \tau_p} = \frac{1}{\gamma} \frac{\partial}{\partial \rho} \left[y^{(1-\gamma)/\gamma} \frac{\partial y}{\partial \rho} \right] + \beta \frac{\partial^2 y}{\partial \rho^2} \quad (6)$$

$$\left[\alpha + \frac{1}{\gamma} y^{(1-\gamma)/\gamma} \right] \frac{\partial y}{\partial \tau_s} = \alpha \frac{\partial^2 y}{\partial \rho^2} \quad (\text{surface diffusion}) \quad (7)$$

The initial and boundary conditions (IC and BC) are given by eq. (8):

$$\left. \begin{array}{l} \text{(IC) } y = 0 \text{ at } \tau_p = 0 \text{ or } \tau_s = 0 \\ \text{(BC) } y = 1 \text{ at } \rho = 0 \quad \partial y / \partial \rho = 0 \text{ at } \rho = 1 \end{array} \right\} \quad (8)$$

Equations (6) and (7) were transformed into finite difference equations and solved numerically.

RESULTS AND DISCUSSION

Figure 2 shows the equilibrium isotherms for the adsorption of C.I. Acid Blue 40 (AB40) and C.I. Acid Red 88 (AR88) onto the cellulose membrane in the single or equimolar binary dye system at

Table I Physical Properties in the Cellulose Membrane–C.I. Acid Blue 40 System at 55°C

Run No.	C_E (mol/m ³)	C_0 (mol/m ³)	α	k	γ	$D'_s \times 10^{12}$ (m ² /s)	$D'_p \times 10^{12}$ (m ² /s)
1	50	0.50	6.73	3.74	0.706	4.60	26.8
2	50	0.80	5.66	3.74	0.706	4.68	22.7
3	50	1.00	5.17	3.74	0.706	4.75	22.5
4	100	0.05	15.8	4.94	0.719	3.04	42.1
5	100	0.10	13.5	4.94	0.719	3.26	38.7
6	100	0.20	10.4	4.94	0.719	3.78	34.3
7	100	0.30	10.6	4.94	0.719	3.72	34.6
8	100	0.50	7.86	4.94	0.719	4.50	29.4
9	150	0.05	20.2	6.36	0.753	2.73	46.8

Table II Physical Properties in the Cellulose Membrane–C.I. Acid Blue 40 in the Presence of C.I. Acid Red 88 at 55°C

Run	C_E (mol/m ³)	C_0 (mol/m ³)	k	α	β	γ	$D'_s \times 10^{12}$ (m ² /s)	$D'_p \times 10^{12}$ (m ² /s)
1	50	0.05	2.97	11.4	0.671	0.643	3.42	33.0
2	50	0.10	2.97	9.29	0.547	0.643	4.07	32.0
3	50	0.30	2.97	6.30	0.371	0.643	5.16	27.4
4	50	0.50	2.97	5.26	0.310	0.643	5.92	26.2
5	100	0.05	4.20	14.6	0.860	0.674	3.19	39.4
6	100	0.10	4.20	12.6	0.742	0.674	3.58	38.0
7	100	0.20	4.20	9.91	0.584	0.674	3.72	31.7
8	100	0.30	4.20	8.92	0.525	0.674	3.92	30.0
9	100	0.50	4.20	6.90	0.604	0.674	4.85	28.6

55°C. Sodium chloride (100 mol/m³) is added to stimulate adsorption. The adsorption isotherms for the binary system revealed Freundlich-type adsorption as well as that of a single dye system. Although the amounts of adsorbed dye for both dyes are similar and small, that for AR88 is a little larger than that for AB40 in the single and mixture systems. Apparently, the amount of equilibrium adsorption for each dye was decreased by the presence of the other dye. Freundlich coefficients (k and γ of $q_0 = kC_0^\gamma$) were determined from the intercepts and slopes of the lines and are summarized in Tables I–III. The value of α in eq. (2) was also determined and is summarized in Tables I–III.

Figure 3 shows the experimental uptake curves for AB40 at different dye concentrations measured by using one sheet of cellulose membrane, which shows the relation between the amount of the dye in one sheet of the cellulose membrane [A'] (mol/kg) and time (min) at 55°C. The bulk-

phase concentration of NaCl (C_E) was 100 mol/m³. The amount of the dye in one sheet of the cellulose membrane depends on the dye concentration in the bulk solution (C_0). The solid and broken lines show the theoretical lines for surface diffusion control [eq. (7)] and pore diffusion control [eq. (6), $\beta = 0$], respectively. The experimental data correlated well with both models. Then, the surface diffusivity based on the surface diffusion control D'_s (m²/s) and the pore diffusivity based on the pore diffusion control D'_p (m²/s) were determined by matching the theoretical values calculated from eqs. (7) and (6) with the data, respectively (see Table I).

As shown in our previous articles,^{9,12} the surface diffusivity of the parallel diffusion model (D_s) can be obtained by plotting D'_s vs. $1/\alpha$; therefore, it was represented by the symbol of circles in Figure 4. The plots of D'_s vs. $1/\alpha$ were correlated well by a line at $\alpha \cong 7.86$. The increase of D'_s with increasing $1/\alpha$ indicates the increasing contribu-

Table III Physical Properties in the Cellulose Membrane–C.I. Acid Red 88 System in the Presence and Absence of C.I. Acid Blue 40 at 55°C

Run	C_E (mol/m ³)	C_0 (mol/m ³)	Mixture System				Single System ¹¹			
			k	α	β	γ	k	α	β	γ
1	50	0.05	3.68	16.8	5.85	0.575	4.17	19.8	6.89	0.551
2	50	0.10	3.68	13.9	4.84	0.575	4.17	14.8	5.15	0.551
3	50	0.30	3.68	8.67	3.02	0.575	4.17	10.1	3.51	0.551
4	50	0.50	3.68	6.90	2.40	0.573	4.17	7.96	2.77	0.551
5	100	0.05	5.72	22.8	7.93	0.600	6.21	25.5	8.87	0.597
6	100	0.10	5.72	18.6	6.47	0.600	6.21	20.1	6.99	0.597
7	100	0.20	5.72	13.9	4.84	0.600	6.21	16.6	5.78	0.597
8	100	0.30	5.72	12.2	4.25	0.600	6.21	14.1	4.91	0.597
9	100	0.50	5.72	9.16	3.19	0.600	6.21	11.8	4.11	0.597

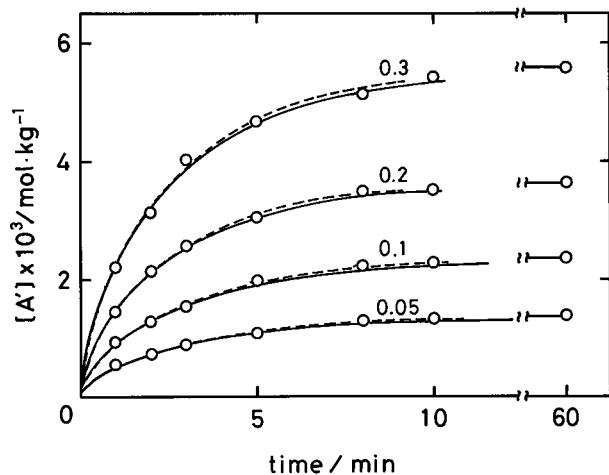


Figure 3 Effects of dye concentration (C_0) on uptake curves of C.I. Acid Blue 40 at 55°C in the presence of 100 mol/m³ of NaCl (C_E) at 55°C. Nos. on the lines represent C_0 (mol/m³): (—) theoretical lines for surface diffusion control [eq. (7)]; (---) theoretical lines for pore diffusion control [eq. (6)].

tion of pore diffusion with decreasing α . The reason that D'_s approaches a constant value at small α is not clear. The surface diffusivity for the parallel diffusion model D_s could be obtained from the intercept of the line and is summarized in Table IV with that for AR88¹¹.

Figure 5 shows the relation between D'_p which was determined assuming the pore diffusion control and α for AB40 by the symbol of circles at 55°C. The plots of D'_p vs. α were correlated well by a line at $\alpha \cong 7.86$. Increasing D'_p with increasing α indicates the increasing contribution of the

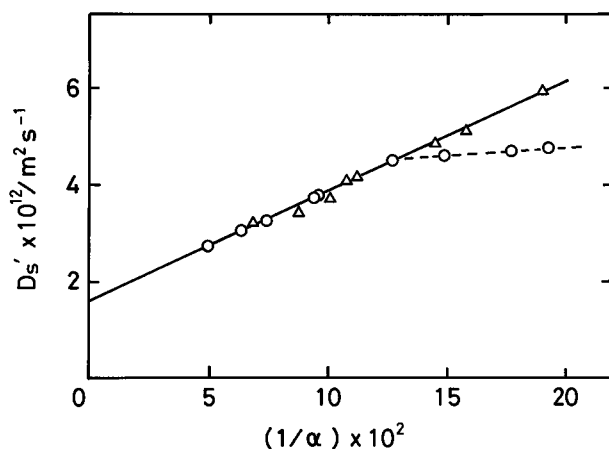


Figure 4 The relation between the surface diffusivity based on surface diffusion control (D'_s) and $1/\alpha$ at 55°C: (○) AB40 single; (△) AB40 in the presence of AR88.

Table IV The Surface and Pore Diffusivities for the Parallel Diffusion Model for C.I. Acid Blue 40 and C.I. Acid Red 88 at 55°C

Dye	$D_s \times 10^{12}$ (m ² /s)	$D_p \times 10^{12}$ (m ² /s)
C.I. Acid Blue 40	1.59	19.5
C.I. Acid Red 88 ¹¹	1.66	4.77

surface diffusion with increasing α . The pore diffusivity for the parallel diffusion model D_p was obtained from the intercept of the line¹⁰ and is summarized in Table IV with that for AR88¹¹. There is little difference in the D_s of both dyes; however, there is big difference in the D_p of both dyes, because AR88 has a strong tendency to self-associate in the solution.¹⁵

Figure 6 shows the uptake curves for AB40 in the presence of the same concentration of AR88. We tried to determine the diffusivity of the dye in the binary mixture under the assumption that the diffusion of AB40 is independent of the existence of AR88. The solid and broken lines until ca. 7–10 min show the theoretical lines for surface diffusion control [eq. (7)] and pore diffusion control [eq. (6), $\beta = 0$] calculated using the values of α and γ in Table II until a 96% fractional attainment of equilibrium, respectively. We assumed that the concentration of the dye anions in the pores is in local equilibrium with the concentration of adsorbed dye anions on the inner surface of the pore wall in assumption (4) of the theory. In the mixture diffusion, the same assumption was adopted and Freundlich coefficients in the

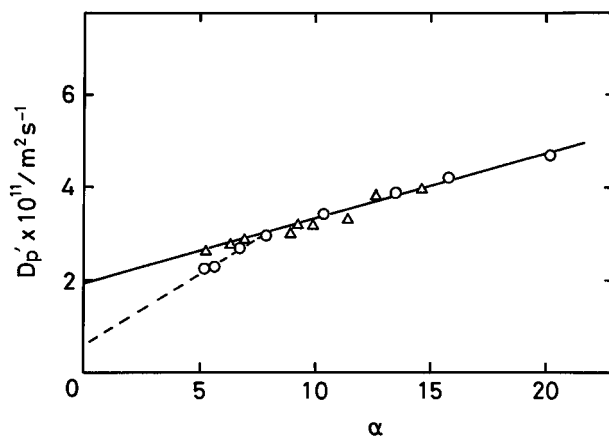


Figure 5 Effects of α on the pore diffusivity based on pore diffusion control (D'_p) at 55°C: (○) AB40 single; (△) AB40 in the presence of AR88.

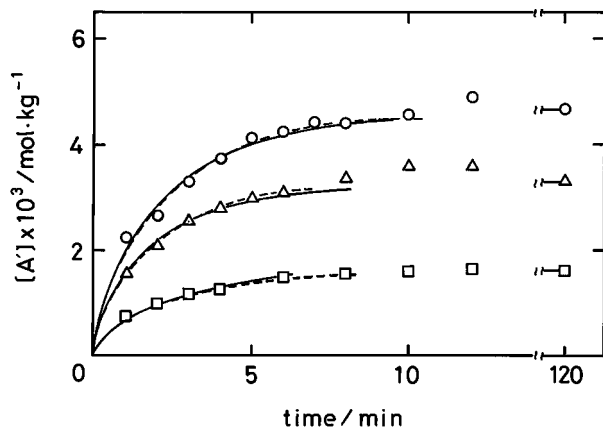


Figure 6 Uptake curves of C.I. Acid Blue 40 in the presence of AR88 at 55°C: (○) $C_0 = 0.3$, $C_E = 100$; (△) $C_0 = 0.3$, $C_E = 50$; (□) $C_0 = 0.1$, $C_E = 50$ (mol/m³). (—) Theoretical lines for surface diffusion control [eq. (7)]; (---) theoretical lines for pore diffusion control [eq. (6)].

mixture system were used. The solid and broken lines show the theoretical lines for the surface diffusion control [eq. (7)] and pore diffusion control [eq. (6), $\beta = 0$], respectively. The experimental data correlated well with both models. Then, the surface diffusivity based on the surface diffusion control D'_s (m²/s) and the pore diffusivity based on the pore diffusion control (m²/s) were determined by matching the theoretical values calculated from eqs. (7) and (6) with the data, respectively (see Table II). The obtained diffusivities for the surface diffusion control D'_s were also plotted vs. $1/\alpha$ by the symbol of angles in Figure 4. They correlated with the line for the single system. On the other hand, the obtained diffusivities for pore diffusion control D'_p were also plotted vs. α in Figure 5. They correlated with the line for the single system. The plots of D'_s and D'_p at $\alpha < 7.86$ correlated well with the lines in Figures 4 and 5. It might be because the total dye concentration in the fiber phase is higher by the contribution of AR88.

Figure 7 shows the uptake curves for AR88 in the presence of the same concentration of AB40 at different concentrations of the dyes and NaCl. The solid lines until ca. 15–18 min represent the theoretical line for the parallel diffusion model [eq. (6)] up to a 96% fractional attainment of equilibrium calculated using the values of α , β , and γ of the mixture system in Table III. The theoretical lines lie below the experimental values from the beginning of the uptake. The experimental values at 10–15 min are larger than are the

values of the equilibrium adsorption. Then, an attempt was made to adopt the data with the theoretical line for the single system. The broken lines represent the theoretical lines for the parallel diffusion model [eq. (6)] up to a 96% fractional attainment of equilibrium calculated using the values of α , β , and γ for the single system in Table III. The lines agreed with the experimental data. This result implies that AR88, which has a higher affinity than that of AB40, diffuses independently of AB40 in a same manner of single dyeing at least up to ca. a 96% fractional attainment of equilibrium. Then, AR88 starts decreasing near the equilibrium where the total amount of dye concentration is increasing and then attains equilibrium.

CONCLUSIONS

Adsorption isotherms and uptake curves for single and mixture dyeing of C.I. Acid Blue 40 (AB40) and/or C.I. Acid Red 88 (AR88) with a lower affinity onto cellulose into a cellulose membrane were measured at 55°C and analyzed on the basis of the parallel diffusion model which was developed in the single system. The following conclusions were made: (1) Amounts of equilibrium adsorption for the dyes decreased in the presence of the other dye. (2) Equilibrium adsorption of both dyes in the mixture could be described

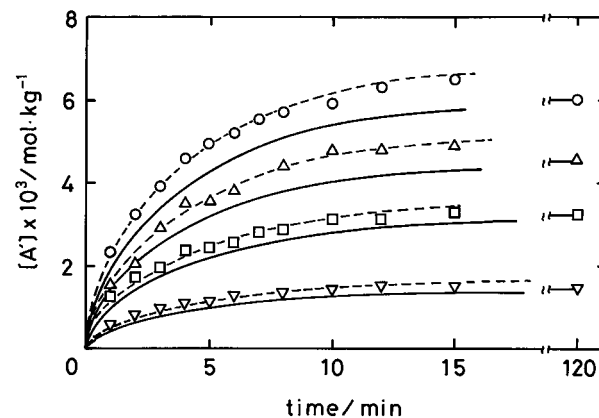


Figure 7 Uptake curves of C.I. Acid Red 88 in the presence of AB40 at 55°C: (○) $C_0 = 0.5$, $C_E = 50$; (△) $C_0 = 0.3$, $C_E = 50$; (□) $C_0 = 0.1$, $C_E = 100$; (▽) $C_0 = 0.05$, $C_E = 50$ (mol/m³). (—) Theoretical lines for the parallel diffusion model using α , β , and γ of a mixture system in Table III [eq. (6)]; (---) theoretical lines for the parallel diffusion model using α , β , and γ of a single system in Table III [eq. (6)].

by the Freundlich equation. (3) The surface and pore diffusivities for the parallel diffusion model of AB40 in the mixture dyeing were the same as those in the single dyeing, in which the dye concentration in the pores was locally in equilibrium with the adsorbed dye concentration according to Freundlich coefficients in mixture dyeing. (4) Diffusion of AR88, which has a higher affinity than that of AB40, was described by the parallel diffusion model with the same diffusivities in the single dyeing, in which dye concentration in the pores was locally in equilibrium with the adsorbed dye concentration according to Freundlich coefficients in single dyeing.

REFERENCES

1. Y. Horiki, Y. Tanizaki, and N. Ando, *Bull. Chem. Soc. Jpn.*, **33**, 163 (1960).
2. Y. Horiki, *Bull. Chem. Soc. Jpn.*, **36**, 1602 (1963).
3. Z. Morita, T. Iijima, and M. Sekido, *J. Appl. Polym. Sci.*, **16**, 407 (1972).
4. A. Johnson, N. M. Patel, and R. H. Peters, *J. Soc. Dyers Colour.*, **90**, 50 (1974).
5. M. Sekido and Z. Morita, *Bull. Chem. Soc. Jpn.*, **35**, 1375 (1962).
6. M. Sekido and Z. Morita, *Bull. Chem. Soc. Jpn.*, **36**, 1602 (1963).
7. H. Yoshida, T. Kataoka, M. Nango, S. Ohta, K. Kuroki, and M. Maekawa, *J. Appl. Polym. Sci.*, **32**, 4185 (1986).
8. H. Yoshida, T. Kataoka, M. Maekawa, and M. Nango, *Chem. Eng. J.*, **41**, B1 (1989).
9. H. Yoshida, M. Maekawa, and M. Nango, *Chem. Eng. Sci.*, **46**, 429 (1991).
10. M. Maekawa, K. Murakami, and H. Yoshida, *J. Colloid Interf. Sci.*, **155**, 79 (1993).
11. M. Maekawa, M. Tanaka, and H. Yoshida, *J. Colloid Interf. Sci.*, **170**, 146 (1995).
12. M. Maekawa, K. Murakami, and H. Yoshida, *Colloid Polym. Sci.*, **273**, 793 (1995).
13. M. Maekawa and M. Kondo, *Colloid Polym. Sci.*, **274**, 1145 (1996).
14. C. Robinson and H. Mills, *Proc. R. Soc. Lond. A*, **131**, 576 (1931).
15. K. Hamada and M. Mitsuishi, *Dyes Pig.*, **16**, 111 (1991).